



# Molecular mechanisms underlying catalytic activity of delta 6 desaturase from *Glossomastix chryso-plasta* and *Thalassiosira pseudonana*<sup>S</sup>

Haisu Shi (史海粟),<sup>1</sup> Rina Wu (乌日娜),<sup>1</sup> Yan Zheng (郑艳), and Xiqing Yue (岳喜庆)

College of Food Science, Shenyang Agricultural University, Shenyang 110866, P.R. China

**Abstract** Delta 6 desaturase (FADS2) is a critical bifunctional enzyme required for PUFA biosynthesis. In some organisms, FADS2s have high substrate specificity, whereas in others, they have high catalytic activity. Previously, we analyzed the molecular mechanisms underlying high FADS2 substrate specificity; in this study, we assessed those underlying the high catalytic activity of FADS2s from *Glossomastix chryso-plasta* and *Thalassiosira pseudonana*. To understand the structural basis of this catalytic activity, GcFADS2 and TpFADS2 sequences were divided into nine sections, and a domain-swapping approach was applied to examine the role of each section in facilitating the catalytic activity of the overall protein. The results revealed two regions essential to this process: one that extends from the end of the fourth to the beginning of the fifth cytoplasmic transmembrane domain, and another that includes the C-terminal region that occurs after the sixth cytoplasmic transmembrane domain. Based on the domain-swapping analyses, the amino acid residues at ten sites were identified to differ between the GcFADS2 and TpFADS2 sequences, and therefore further analyzed by site-directed mutagenesis. T302V, S322A, Y375F, and M384S/M385 substitutions in TpFADS2 significantly affected FADS2 catalytic efficiency.<sup>1</sup> This study offers a solid basis for in-depth understanding of catalytic efficiency of FADS2.—Shi, H., R. Wu, Y. Zheng, and X. Yue. **Molecular mechanisms underlying catalytic activity of delta 6 desaturase from *Glossomastix chryso-plasta* and *Thalassiosira pseudonana*.** *J. Lipid Res.* 2018. 59: 79–88.

**Supplementary key words** polyunsaturated fatty acids • catalytic activity • eicosapentaenoic acid • chimera •  $\alpha$ -linolenic acid

Both linoleic acid (LA, 18:2 <sup>$\Delta$ 9,12</sup>) and  $\alpha$ -linolenic acid (ALA, 18:3 <sup>$\Delta$ 9,12,15</sup>) are essential for human health but cannot be synthesized by the body, and therefore must be obtained from dietary sources (1). Delta 6 fatty acid desaturase (FADS2) is a critical enzyme in the fatty acid biosynthesis pathway that controls the conversion of LA and ALA to

$\gamma$ -linolenic acid (GLA, 18:3 <sup>$\Delta$ 6,9,12</sup>) and stearidonic acid (SDA, 18:4 <sup>$\Delta$ 6,9,12,15</sup>), respectively (2–4). The level of FADS2 catalytic activity determines the rate at which LA and ALA are converted as well as the volume and type of products produced. For example, whereas the body generally converts ALA to EPA (20:5 <sup>$\Delta$ 5,8,11,14,17</sup>) and EPA to DHA (22:5 <sup>$\Delta$ 4,7,10,13,16,19</sup>) at a low rate (5–8), a high level of endogenous FADS2 catalytic activity promotes the production of long-chain PUFAs, such as arachidonic acid (AA, 20:4 <sup>$\Delta$ 5,8,11,14</sup>), and EPA from LA and ALA, respectively. This is evident from the fact that various organisms harbor FADS2s with high or low catalytic activity for LA and ALA as a result of differences in their *FADS2* gene and/or amino acid sequences.

Presumably, these differences mainly occur within the FADS2 substrate-binding and/or catalytic domain(s) that determine its substrate specificity and catalytic activity, respectively. Specifically, a substrate can only be catalyzed by the FADS2 catalytic domain(s) after having been bound by the FADS2 binding domain(s). A previous study by our research group analyzed the molecular mechanisms underlying FADS2 substrate specificity and confirmed the FADS2 substrate-binding domains (9). Notably, the catalytic activity of the generated chimera FADS2s was much lower than that exhibited by the analyzed wild-type FADS2s, likely due to incurred disruptions of the three-dimensional structures of their catalytic domains. Thus, the present study further investigated the molecular mechanisms mediating FADS2 catalytic activity in *Thalassiosira pseudonana* and *Glossomastix chryso-plasta*.

A comparison of the FADS2 catalytic efficiency for ALA in various species (supplemental Table S1) revealed that the marine microalgae, *T. pseudonana*, which exhibits a strong capacity for EPA and DHA production, exhibits high

Abbreviations: AA, arachidonic acid (20:4 <sup>$\Delta$ 5,8,11,14</sup>); ALA,  $\alpha$ -linolenic acid (18:3 <sup>$\Delta$ 9,12,15</sup>); FADS2, delta 6 desaturase; GLA,  $\gamma$ -linolenic acid (18:3 <sup>$\Delta$ 6,9,12</sup>); LA, linoleic acid (18:2 <sup>$\Delta$ 9,12</sup>); SDA, stearidonic acid (18:4 <sup>$\Delta$ 6,9,12,15</sup>).

<sup>1</sup>To whom correspondence should be addressed.

e-mail: wrn6956@163.com (R.W.); shihaisu@syau.edu.cn (H.S.)

<sup>S</sup>The online version of this article (available at <http://www.jlr.org>) contains a supplement.

This study was supported by the National Natural Science Foundation of China (No. 31471713).

Manuscript received 9 August 2017 and in revised form 15 November 2017.

Published, JLR Papers in Press, November 22, 2017

DOI <https://doi.org/10.1194/jlr.M079806>

Copyright © 2018 by the American Society for Biochemistry and Molecular Biology, Inc.

This article is available online at <http://www.jlr.org>

FADS2 (TpFADS2) catalytic efficiency for both LA and ALA compared with other plants and fungi. Specifically, its conversion efficiency is 68% for LA in the  $\omega$ -6 pool, and 80% for ALA in the  $\omega$ -3 pool; however, this high catalytic efficiency is associated with low specificity (supplemental Table S1) for both substrates. In contrast, the stramenopile marine microalga, *G. chrysoiplasta*, also produces a high level (46%) of EPA but exhibits a FADS2 (GcFADS2) with a limited ability to convert LA to GLA, and ALA and SDA, only achieving a conversion efficiency of 6% and 7%, respectively. Moreover, GcFADS2 also exhibits a low substrate specificity for both substrates (supplemental Table S1).

Although various research groups have previously cloned and sequenced the FADS2 genes of many organisms (10–18), and our own group previously analyzed the molecular mechanism underlying FADS2 substrate specificity (9), it is still not clear which key domain and/or amino acid mediates FADS2 catalytic activity. This is largely a reflection of the fact that, to date, no information is available regarding the FADS2 crystal structure; however, Wang et al. (19) and Bai et al. (20) recently analyzed the crystal structure of human and mammalian FADS9 (delta 9 desaturase), respectively. The results of their analyses showed the three-dimensional FADS9 structure to be mushroom-shaped, and revealed key FADS9-binding and catalytic sites for the first time.

In the present study, TpFADS2 and GcFADS2 genes were synthesized and their catalytic activity for LA and ALA then characterized in *Saccharomyces cerevisiae*. Furthermore, the TpFADS2 and GcFADS2 domains were recombined to produce various chimeras that were subsequently expressed in *S. cerevisiae*, to enable identification of the location of key sequence regions essential for substrate catalysis. Finally, site-directed mutagenesis was targeted to these key regions to confirm sites essential for FADS2 catalytic activity.

## MATERIALS AND METHODS

### Strains and plasmids

TpFADS2 (GenBank accession AY817155) and GcFADS2 (GenBank accession AAU11445) genes were synthesized by Shanghai Sunny Biotechnology Co. Ltd; INVSc1 yeast strain (Invitrogen) was used for heterogeneous expression and catalytic activity determination for TpFADS2, GcFADS2, and each chimera. Plasmid pYES2/NT C (Invitrogen) was used for each chimera expression.

### Media and gene synthesis

LB agar plates and SC-Uracil synthetic minimal medium was used as described previously (9). Codon optimized TpFADS2 and GcFADS2 genes were synthesized and subcloned into the vector pUC57 and transformed into *Escherichia coli* Top 10.

### Primer design, PCR amplification and sequence analysis for GcFADS2 and TpFADS2

For TpFADS2 and GcFADS2 gene amplification, primers were synthesized based on TpFADS2 and GcFADS2 gene sequences. The forward primers were FTp and FGc and the reverse primers were RTp and RGc (all primers are listed in supplemental Table S1). After initial denaturation at 95°C for 5 min, PCR amplification was performed in 30 cycles of 50 s at 95°C, 50 s at 58°C, and

2 min at 68°C, followed by a final extension at 68°C for another 10 min. The recombinant plasmids designated pYES2-GcFADS2 and pYES2-TpFADS2 were constructed as described previously (9).

### Construction of each chimeric gene by reciprocal section swapping

According to the transmembrane topology of FADS2 (hydrophilic regions and hydrophobic regions), GcFADS2 and TpFADS2 genes were divided into nine regions (Fig. 1). To determine catalytic activity of each region, the corresponding regions of both FADS2 enzymes were systematically exchanged to construct recombinant swap genes, which were generated by overlap extension PCR with the primers listed in supplemental Table S1. The protocol of PCR used was the same as described previously (9). The hybrid genes were ligated into the pYES2 plasmid and transformed into competent Top10 cells.

### Site-directed mutagenesis of GcFADS2

For site-directed mutagenesis, oligonucleotide primers were used to introduce nucleotide substitutions into TpFADS2 using the Fast Site-Directed Mutagenesis Kit. Ten mutants derived from the GcFADS2 gene were constructed, where amino acids were substituted with the corresponding residues in the TpFADS2 gene (V295T, T299S, L303F, I306L, A315S, H360D, F368Y, S377M/L378M, H381N, and L383I). Mutation primers are listed in supplemental Table S1.

### Yeast transformation, heterologous expression in *S. cerevisiae*, and measurement of chimeric desaturase activity for LA and ALA

Constructs pYES2-Chimera 1~18, pYES2-TpFADS2 and pYES2-GcFADS2 were transformed into *S. cerevisiae*. GcFADS2 and TpFADS2 genes were induced under the conditions described previously (9). Then the expression level of each chimeric desaturase in *S. cerevisiae* was determined by Western blotting analysis as described previously (9).

### Lipid extraction and fatty acid analysis

Lipids from an equivalent weight of cells were extracted and methyl-esterified, and fatty acid content was analyzed by GC as described previously (21).

### Kinetic analysis

Kinetic studies were carried out using 0.25 or 0.5 mM *cis*-LA/ALA substrate. The substrate was added to the induced medium for 12 h (720 min).  $V_{max}$  and  $K_m$  values of each recombinant TpFADS2 and GcFADS2 by mutating amino acids were calculated by the Michaelis-Menten equation.

### Topology prediction

The predicted topology model for GcFADS2 and TpFADS2 was performed with prediction of transmembrane helices in proteins (Fig. 2). The domain responsible for substrate specificity of FADS2s analyzed previously was described together with the region responsible for their catalytic activity in one predicted topology model.

## RESULTS

### Cloning and characterization of TpFADS2 and GcFADS2

To characterize the catalytic activities of TpFADS2 and GcFADS2, 1452- and 1395-bp DNA fragments were amplified using FTp/RTp and FGc/RGc primers, respectively (supplemental Table S1). After their (pYES2-TpFADS2 and pYES2-GcFADS2) successful expression was confirmed

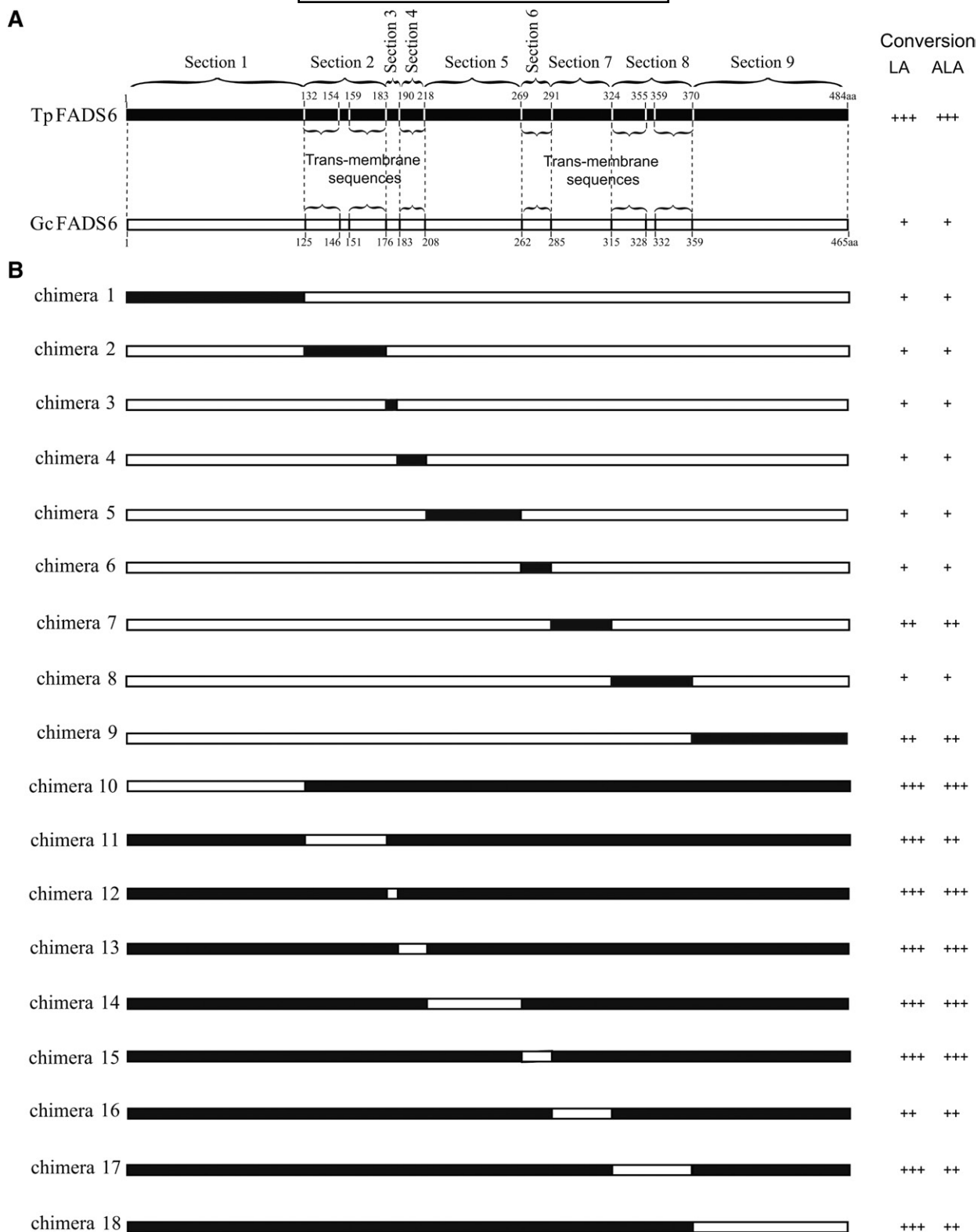


**Fig. 1.** A: Skeleton map of the amino acid sequences of TpFADS2 (black bar) and GcFADS2 (white bar), which were divided into 9 sections shown by dotted lines. The braces indicate their trans-membrane sequences. B: Map of each FADS2 chimera constructed by reciprocal section swapping. Regions in black bars originated from TpFADS2 and regions in white bars originated from GcFADS2. Substrate conversion efficiency of each chimera was classified into three groups: +, <10%; ++, 11–25%; +++, >26%.

via Western blot analysis, the generated constructs were incubated with fatty acid substrates. As a result, TpFADS2 was shown to convert LA and ALA at a rate of  $65.6 \pm 1.8\%$  and  $77.6 \pm 1.9\%$ , respectively, while conversely, GcFADS2 only

catalyzed the conversion of LA and ALA at a rate of  $5.6 \pm 0.8\%$  and  $7.6 \pm 0.6\%$ , respectively (**Table 1**). These results are consistent with those previously reported by Hsiao et al. (10) and Tonon et al. (22).

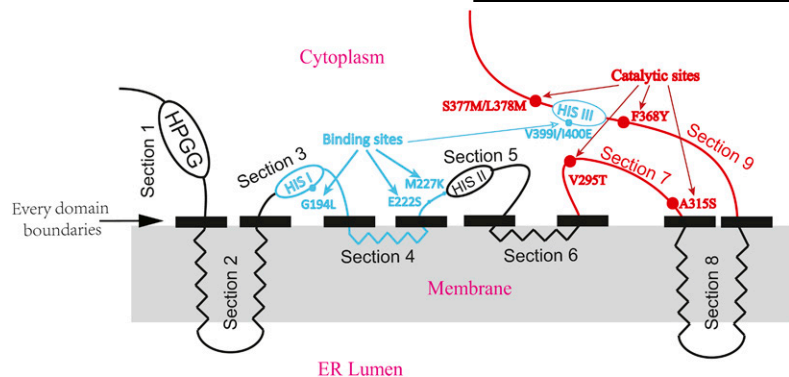


**Fig. 2.** The predicted topology model of FADS2. Four transmembrane  $\alpha$ -helices span the ER lumen and the other polypeptides extend into the cytoplasm. Black solid rectangles indicate each domain boundary. Blue lines and blue dots indicated the areas and sites influencing substrate specificity from our previous work, whereas red lines and red dots indicated the key areas and sites influencing catalytic activity, respectively. ER lumen: endoplasmic reticulum lumen.

### Multiple sequence alignment of the FADS2s

The cloned GcFADS2 amino acid sequence was shown to share 51.87% identity with that of TpFADS2. To determine the structural basis for FADS2 catalytic activity, a multiple sequence alignment was performed to compare several FADS2s, which were arranged according to their capacity for ALA catalytic activity (i.e., such that those with a stronger catalytic activity for ALA were placed above those with a weaker ALA catalytic activity). The FADS2s with high catalytic activity were expected to share a homologous fragment/site that was absent from the sequences of those with low catalytic activity; however, the results of the conducted alignment result failed to identify such a fragment or site (supplemental Fig. S1).

### Construction and expression of fusion genes in yeast

To identify which structural elements are functionally involved in TpFADS2 and GcFADS2 catalytic activity, each enzyme was divided into nine sections as follows: Section 1, the N-terminal end region before the first cytoplasmic transmembrane domain; Section 2, the first and second transmembrane domains; Section 3, the region extending from the end of the second transmembrane domain to the beginning of the third cytoplasmic transmembrane domain; Section 4, the third transmembrane domain; Section 5, the region extending from the end of the third transmembrane domain to the beginning of the fourth cytoplasmic

transmembrane domain; Section 6, the fourth transmembrane domain; Section 7, the region extending from the end of the fourth transmembrane domain to the beginning of the fifth cytoplasmic transmembrane domain; Section 8, the fifth and sixth transmembrane domains; Section 9, the C-terminal region following the sixth cytoplasmic transmembrane domain (Fig. 2). The expression levels of the 18 generated chimeras in *S. cerevisiae* were then quantified via Western blot analysis, and the molecular weight of each was confirmed to be consistent with that predicted (Fig. 3).

### Locating key FADS2 catalytic activity domains

The catalytic activity of each construct was next determined by measuring the levels of the remaining substrate and conversion products present in lipids extracted from the transfected *S. cerevisiae* cells. The results of this analysis showed that while the catalytic efficiency of GcFADS2 was  $5.6 \pm 0.8\%$  and  $7.6 \pm 0.6\%$  for LA and ALA respectively, that of chimera 7 (GcFADS2 aa285-315 replaced by TpFADS2 aa291-324) was increased to  $25.0 \pm 1.3\%$  and  $35.3 \pm 3.5\%$ , respectively. Conversely, where TpFADS2 exhibited a catalytic efficiency of  $22.6 \pm 2.6\%$  and  $15.3 \pm 0.9\%$ , for LA and ALA, respectively, that of chimera 16 (TpFADS2 aa291-324 replaced by GcFADS2 aa285-315) was decreased to  $65.6 \pm 1.8\%$  and  $77.6 \pm 1.9\%$ , respectively. The catalytic efficiency of chimera 9 (GcFADS2 aa359-458 replaced by TpFADS2

**TABLE 1.** Fatty acid compositions (% w/w) of the total lipid contents of yeast transformants harboring the control plasmid (pYES2) and the recombinant plasmids (pYES2-GcFADS2 and pYES2-TpFADS2) by adding 0.5 mM *cis*-LA or 0.5 mM *cis*-ALA or both substrates (0.25 mM *cis*-LA and 0.25 mM *cis*-ALA substrates)

Fatty acid	Transformants								
	pYES2 (control)			pYES2-GcFADS2			pYES2-TpFADS2		
	+LA <sup>a</sup>	+ALA <sup>a</sup>	+LA and +ALA	+LA	+ALA	+LA and +ALA	+LA	+ALA	+LA and +ALA
16:0 (PA)	21.9 ± 0.5	22.6 ± 0.3	23.6 ± 0.7	25.6 ± 0.1	23.5 ± 0.1	22.2 ± 0.5	22.2 ± 0.2	23.7 ± 0.5	25.5 ± 0.6
16:1 (PA)	10.6 ± 0.2	11.7 ± 0.6	12.6 ± 0.3	11.3 ± 0.6	12.7 ± 0.3	11.1 ± 0.3	11.5 ± 0.1	13.3 ± 0.3	12.6 ± 0.5
18:0 (SA)	10.2 ± 0.5	8.8 ± 0.5	9.3 ± 0.2	9.5 ± 0.3	9.6 ± 0.5	10.5 ± 0.6	9.3 ± 0.3	10.5 ± 0.5	9.3 ± 0.3
18:1 (OA)	11.3 ± 0.5	12.5 ± 0.3	11.6 ± 0.2	13.1 ± 0.2	9.9 ± 0.2	12.2 ± 0.5	9.6 ± 0.6	10.2 ± 0.6	11.1 ± 0.5
18:2 (LA, $\omega$ -6)	40.3 ± 0.3	ND	22.1 ± 0.5	38.0 ± 0.2	ND	18.1 ± 0.4	17.6 ± 0.3	ND	7.2 ± 0.4
18:3 (ALA, $\omega$ -3)	ND	39.5 ± 0.2	21.5 ± 0.8	ND	37.4 ± 1.0	20.1 ± 0.3	ND	15.2 ± 0.6	5.0 ± 0.6
18:3 (GLA, $\omega$ -6)	ND	ND	ND	1.9 ± 0.1	ND	1.1 ± 0.3	22.2 ± 0.5	ND	13.0 ± 0.5
18:4 (SDA, $\omega$ -3)	ND	ND	ND	ND	2.8 ± 0.4	1.6 ± 0.1	ND	24.9 ± 0.9	15.5 ± 0.8
LA conversion rate <sup>b</sup>	—	—	—	4.9 ± 0.1	—	5.6 ± 0.8	55.6 ± 1.4	—	65.6 ± 1.8
ALA conversion rate <sup>b</sup>	—	—	—	—	7.1 ± 0.5	7.6 ± 0.6	—	62.3 ± 0.7	77.6 ± 1.9

<sup>a</sup>There was no significantly difference in LA and ALA conversion rate between single- and double- substrate supplementation.

<sup>b</sup>Conversion rate =  $100 \times ([\text{product}] / [\text{product} + \text{substrate}])$ . ND, not detected; —, none.

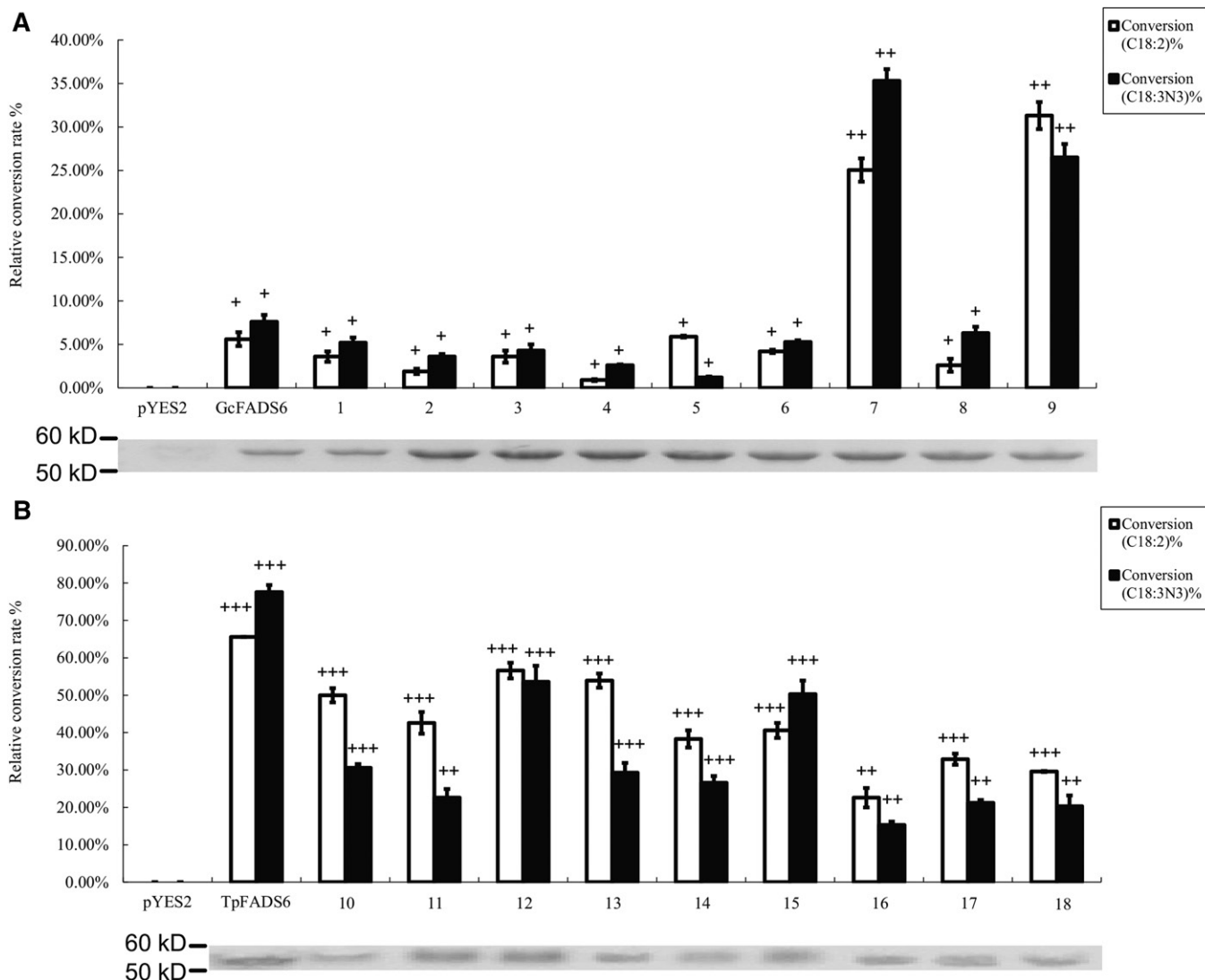


**Fig. 3.** Relative substrate conversion efficiency of each FADS2 chimera expressed in *S. cerevisiae*, determined by adding both substrates. Relative substrate conversion rate =  $100 \times ([\text{product}] / [\text{product} + \text{substrate}]) / \text{density}_{\text{WB}}$ . Density<sub>WB</sub> is the optical density value of Western blotting. Western blotting of recombinant gene expression in *S. cerevisiae* is below each histogram of conversion rate. The number under the abscissa indicates corresponding chimera. A: substrate conversion efficiency and Western blotting of chimera 1–9; B: substrate conversion efficiency and western blotting of chimera 10–18.

aa370–484) for LA and ALA increased to  $31.3 \pm 1.5\%$  and  $26.5 \pm 4.0\%$ , respectively. Finally, the replacement of the aa359–458 region of GcFADS2 resulted in a significant reduction in catalytic activity against both substrates, such that chimera 18 exhibited a catalytic efficiency of  $19.6 \pm 0.2\%$  and  $10.3 \pm 2.9\%$  for LA and ALA, respectively, which represented the lowest rate observed among the TpFADS2 chimeras (chimeras 10–18) (Fig. 3). No other chimeras exhibited a significantly different catalytic efficiency for LA and/or ALA compared with that exhibited by GcFADS2/TpFADS2. These results suggest that the amino acids in sections 7 and 9 of FADS2 likely critically mediate its catalytic activity.

#### Localizing second-level areas within the key FADS2 catalytic activity domains

To further identify key functional areas within sections 7 and 9, section 9 was equally divided into three ‘second-

level’ sections, which were systematically exchanged with a second-level section 7 region between GcFADS2 and TpFADS2, to produce additional recombinant gene sequences (Fig. 4). The results of an analysis of the generated second-level chimeras showed that the catalytic efficiency of chimera 7-1 (“VRALAF” in GcFADS2 replaced by “PYSIMY” in TpFADS2) for both LA and ALA was increased to  $16.6 \pm 0.6\%$  and  $15.2 \pm 0.3\%$ , respectively, compared with that exhibited by GcFADS2 (Fig. 5A). Likewise, replacement of aa359–383 (section 9-1) of GcFADS2 with aa370–394 of TpFADS2 resulted in a significantly increased ( $25.6 \pm 1.9\%$  and  $24.6 \pm 1\%$  for LA and ALA, respectively) catalytic efficiency for both substrates (Fig. 5B). Replacement of the other two second-level sections (sections 9-2 and 9-3) of GcFADS2 had no significant impact on its catalytic efficiency for either substrate (Fig. 5B).

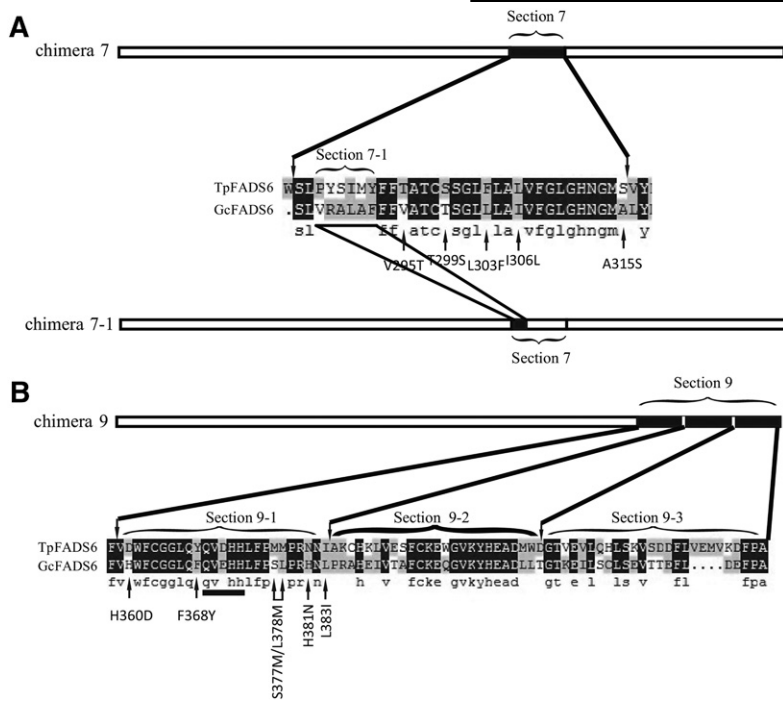


**Fig. 4.** A partial comparison of sections 7 and 9 between GcFADS2- and TpFADS2-deduced amino acids. Section 7-1 indicates the different area between GcFADS2- and TpFADS2-deduced amino acids. Section 9 was equally divided into 3 second-level sections, denoted section 9-1, section 9-2, and section 9-3. Arrows below the alignment indicate the amino acid positions that were selected for site-directed mutagenesis.

### Identifying amino acids that critically mediate FADS2 catalytic activity

To further understand the molecular mechanism underlying FADS2 catalytic activity, a series of constructs with mutations within sections 7 and 9-1 was next generated (Fig. 4). The LA and ALA conversion efficiencies were subsequently shown to be greatly reduced in the single mutants V295T, A315S, and F368Y, as well as the double mutant S377M/L378M, to a rate of  $15.9 \pm 0.5\%$ ,  $15.6 \pm 0.7\%$ ,  $22.6 \pm 0.1\%$ , and  $13.6 \pm 0.6\%$ , respectively, for LA, and  $11.2 \pm 0.1\%$ ,  $5.3 \pm 1.3\%$ ,  $26.3 \pm 0.7\%$ , and  $15.2 \pm 0.3\%$ , respectively, for ALA (Fig. 6A). Targeted mutagenesis of T299S, L303F, I306L, H360D, H381N, and L383I did not induce any major changes to FADS2 catalytic activity for either substrate (Fig. 6A). Conversely, the catalytic efficiency for both substrates was significantly enhanced in the single mutants T302V, S322A, and Y375F, as well as the double mutant M384S/M385L (Fig. 6B). These results suggest that the T302, S322, Y375, and M384/

M385 substitutions in TpFADS2 (corresponding to the V295, A315, F368, and S377/L378 substitutions in GcFADS2) likely alter FADS2 activity because these regions play an important role in FADS2 catalytic activity. Furthermore, by analyzing the effect of substrate concentration on catalytic activity, the catalytic efficiency of all wild-type and mutant FADS2s was shown to be slightly reduced upon exposure to 0.25 mM compared with 0.5 mM cis-LA/ALA. In contrast, the sites identified to critically influence FADS2 catalytic activity remained consistent at all analyzed fatty acid concentrations (Tables 2, 3).

### Kinetics of each mutant desaturase

The affinity of each recombinant TpFADS2/GcFADS2 was next assessed by evaluating their reaction rates in the presence of varying fatty acid concentrations, (where  $V_{max}$  and  $K_m$  were calculated using the Michaelis-Menten equation) (Tables 2, 3). The results of this analysis showed that the  $K_m$  values for both substrates that were exhibited by the single

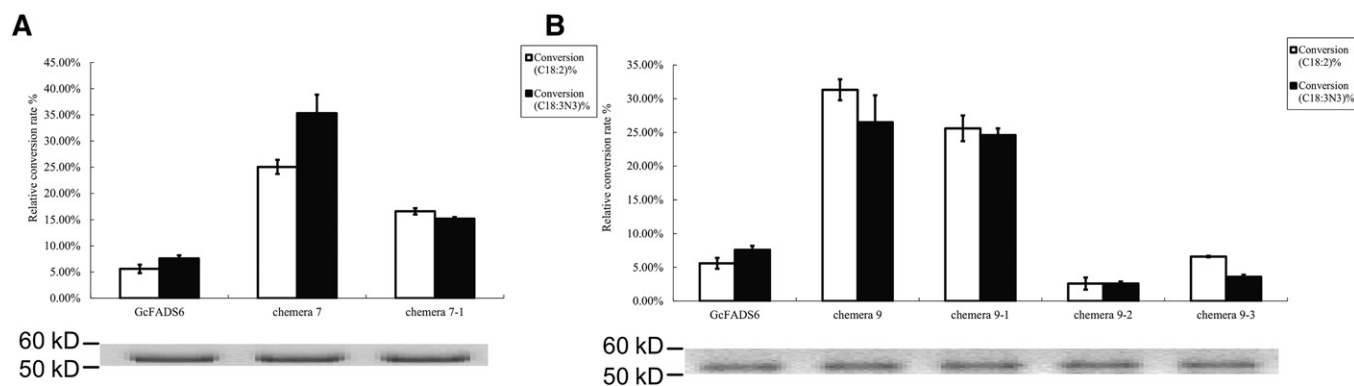


**Fig. 5.** Relative substrate conversion efficiency of chimeras 7-1, 9-1, 9-2, and 9-3 expressed in *S. cerevisiae*, determined by adding both substrates. Relative substrate conversion rate =  $100 \times ([\text{product}] / [\text{product} + \text{substrate}]) / \text{density}_{\text{WB}}$ . Western blotting of recombinant gene expression in *S. cerevisiae* is below each histogram of conversion rate. A: chimera 7-1; B: chimeras 9-1, 9-2, and 9-3.

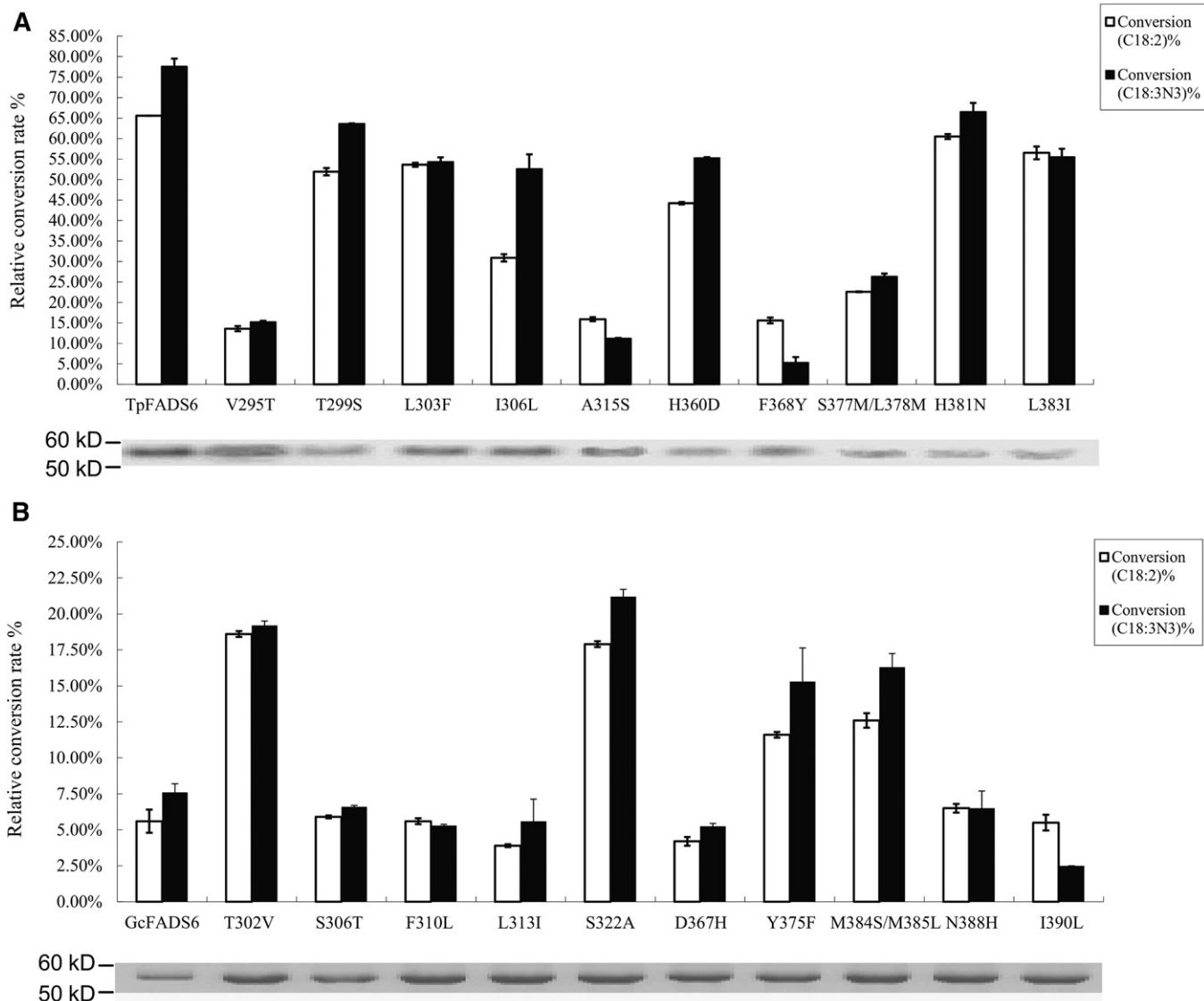


**Fig. 6.** Relative substrate conversion efficiency of each mutant from section 7 and section 9-1. Relative substrate conversion rate =  $100 \times ([\text{product}] / [\text{product} + \text{substrate}]) / \text{density}_{\text{WB}}$ . Western blotting of recombinant gene expression in *S. cerevisiae* is below each histogram of conversion rate. A: Each mutant from TpFADS2; B: each mutant from GcFADS2. The mutants of V295T, T299S, L303F, I306L, A315S, H360D, F368Y, S377M/L378M, H381N, and L383I from TpFADS2 correspond to the mutants of T302V, S306T, F310L, L313I, S322A, D367H, Y375F, M384S/M385L, N388H, and I390L from GcFADS2, respectively.

mutants, V295T, A315S, and F368Y, as well as the double mutant, S377M/L378M, were much higher than those exhibited by the other TpFADS2 mutants. Conversely, the  $K_m$  values were markedly decreased in the single GcFADS2 mutants T302V, S322A, and Y375F, and the GcFADS2 double mutant M384S/M385L, compared with those exhibited by the corresponding TpFADS2 (by a factor of ten) and GcFADS2 mutants (Table 4). Together, these results suggest that of all the mutant constructs, the four mutant GcFADS2 desaturases, T302V, S322A, Y375F, and M384S/M385L, had the strongest affinity for both substrates.

## DISCUSSION

The results of the present study indicate that the FADS2 cytoplasmic region extending from the end of the fourth

transmembrane domain to the beginning of the fifth transmembrane domain (section 7) critically mediates FADS2 catalytic activity (Figs. 4A, 5A). Comparing the GcFADS2 and TpFADS2 sequences within this segment revealed one variant area (“VRALAF” in GcFADS2 and “PYSIMY” in TpFADS2) that includes five different sites. These are 295V, 299T, 303L, 306I, and 315A in GcFADS2, and 302T, 306S, 310F, 313L, and 322S in TpFADS2 (Fig. 4). Of the mutants that included this area and these sites, chimera 7-1, which harbored both V295T and A315S, displayed a large decrease in its conversion rate for both substrates (Fig. 5). The topological model of FADS2 suggests that both 295V and 315A are located in the cytoplasm (Fig. 2), and are likely closely associated with FADS2 catalytic activity. It may be that sites 302T and 322S in TpFADS2 (which correspond to 295V and 315A in GcFADS2) strongly influence

TABLE 2. Fatty acid generation (mM) by yeast transformants expressing the wild-type and the mutant desaturases from TpFADS2

Fatty acid	Mutants										
	TpFADS2	V295T	T299S	L303F	I306L	A315S	H360D	F368Y	S377M/L378M	H381N	L383I
0.25 mM <i>cis</i> -LA/ALA:											
18:2 (LA)	0.081 ± 0.005	0.212 ± 0.002	0.124 ± 0.002	0.110 ± 0.001	0.170 ± 0.002	0.219 ± 0.001	0.149 ± 0.001	0.219 ± 0.002	0.199 ± 0.000	0.090 ± 0.002	0.100 ± 0.004
18:3 (ALA)	0.050 ± 0.005	0.219 ± 0.001	0.099 ± 0.000	0.119 ± 0.003	0.110 ± 0.009	0.228 ± 0.000	0.119 ± 0.001	0.230 ± 0.003	0.188 ± 0.002	0.089 ± 0.006	0.119 ± 0.005
18:3 (GLA)	0.164 ± 0.002	0.034 ± 0.002	0.130 ± 0.001	0.134 ± 0.002	0.077 ± 0.001	0.040 ± 0.001	0.111 ± 0.002	0.039 ± 0.000	0.057 ± 0.002	0.151 ± 0.004	0.141 ± 0.002
18:4 (SDA)	0.194 ± 0.001	0.038 ± 0.000	0.159 ± 0.003	0.136 ± 0.009	0.132 ± 0.000	0.028 ± 0.001	0.138 ± 0.003	0.013 ± 0.002	0.066 ± 0.006	0.166 ± 0.005	0.139 ± 0.000
LA % <sup>a</sup>	65.6 ± 1.8	13.6 ± 0.6	51.9 ± 0.9	53.6 ± 0.5	30.9 ± 0.9	15.9 ± 0.5	44.2 ± 0.3	15.6 ± 0.7	22.6 ± 0.1	60.5 ± 0.6	56.5 ± 1.5
ALA % <sup>a</sup>	77.6 ± 1.9	15.2 ± 0.3	63.6 ± 0.1	54.3 ± 1.1	52.6 ± 3.5	11.2 ± 0.1	55.3 ± 0.2	5.3 ± 1.3	26.3 ± 0.7	66.5 ± 2.2	55.5 ± 2.0
0.5 mM <i>cis</i> -LA/ALA:											
18:2 (LA)	0.299 ± 0.009	0.449 ± 0.001	0.290 ± 0.000	0.317 ± 0.002	0.377 ± 0.000	0.439 ± 0.002	0.340 ± 0.002	0.420 ± 0.001	0.384 ± 0.000	0.286 ± 0.000	0.290 ± 0.005
18:3 (ALA)	0.249 ± 0.008	0.425 ± 0.000	0.240 ± 0.002	0.290 ± 0.002	0.299 ± 0.017	0.459 ± 0.004	0.286 ± 0.004	0.465 ± 0.006	0.389 ± 0.001	0.240 ± 0.010	0.285 ± 0.007
18:3 (GLA)	0.209 ± 0.001	0.060 ± 0.000	0.202 ± 0.002	0.193 ± 0.000	0.113 ± 0.002	0.070 ± 0.002	0.152 ± 0.001	0.072 ± 0.000	0.106 ± 0.000	0.204 ± 0.005	0.204 ± 0.000
18:4 (SDA)	0.259 ± 0.000	0.065 ± 0.002	0.251 ± 0.002	0.203 ± 0.017	0.210 ± 0.004	0.049 ± 0.004	0.204 ± 0.006	0.025 ± 0.001	0.120 ± 0.010	0.251 ± 0.007	0.205 ± 0.000
LA % <sup>a</sup>	41.8 ± 1.8	11.9 ± 0.2	40.4 ± 0.1	38.5 ± 0.4	22.6 ± 0	14 ± 0.4	30.4 ± 0.3	14.3 ± 0.3	21.2 ± 0	40.8 ± 0.1	40.7 ± 0.9
ALA % <sup>a</sup>	51.8 ± 1.7	13 ± 0.1	50.3 ± 0.3	40.7 ± 0.3	42 ± 3.4	9.8 ± 0.7	40.8 ± 0.8	5 ± 1.1	23.9 ± 0.1	50.2 ± 1.9	41 ± 1.4

<sup>a</sup>LA % or ALA % = 100 × ([product] / [product + substrate]).

TABLE 3. Fatty acid concentration (mM) of yeast transformants expressing the wild-type and the mutant desaturases from GcFADS2

Fatty acid	Mutants										
	GcFADS2	T302V	S306T	F310L	L313I	S322A	D367H	Y375F	M384S/M385L	N388H	I390L
0.25 mM <i>cis</i> -LA/ALA:											
18:2 (LA)	0.220 ± 0.002	0.209 ± 0.001	0.235 ± 0.000	0.220 ± 0.001	0.239 ± 0.000	0.205 ± 0.001	0.239 ± 0.001	0.219 ± 0.000	0.219 ± 0.001	0.234 ± 0.001	0.236 ± 0.001
18:3 (ALA)	0.229 ± 0.002	0.209 ± 0.001	0.244 ± 0.000	0.245 ± 0.000	0.245 ± 0.004	0.170 ± 0.001	0.226 ± 0.001	0.206 ± 0.006	0.208 ± 0.002	0.206 ± 0.003	0.235 ± 0.000
18:3 (GLA)	0.014 ± 0.001	0.047 ± 0.000	0.015 ± 0.001	0.014 ± 0.000	0.01 ± 0.001	0.045 ± 0.001	0.011 ± 0.000	0.029 ± 0.001	0.032 ± 0.001	0.016 ± 0.001	0.014 ± 0.000
18:4 (SDA)	0.019 ± 0.001	0.048 ± 0.000	0.017 ± 0.000	0.013 ± 0.004	0.014 ± 0.001	0.053 ± 0.001	0.013 ± 0.006	0.038 ± 0.002	0.041 ± 0.003	0.016 ± 0.000	0.006 ± 0.000
LA % <sup>a</sup>	5.6 ± 0.8	18.6 ± 0.2	5.9 ± 0.1	5.6 ± 0.2	3.9 ± 0.1	17.9 ± 0.2	4.2 ± 0.3	11.6 ± 0.2	12.6 ± 0.5	6.5 ± 0.3	5.5 ± 0.5
ALA % <sup>a</sup>	7.6 ± 0.6	19.2 ± 0.3	6.6 ± 0.1	5.3 ± 0.1	5.6 ± 1.5	21.2 ± 0.5	5.25 ± 0.2	15.3 ± 2.3	16.3 ± 0.9	6.5 ± 1.2	2.5 ± 0.2
0.5 mM <i>cis</i> -LA/ALA:											
18:2 (LA)	0.470 ± 0.001	0.459 ± 0.001	0.465 ± 0.004	0.466 ± 0.001	0.474 ± 0.000	0.454 ± 0.000	0.472 ± 0.001	0.460 ± 0.002	0.450 ± 0.002	0.479 ± 0.001	0.464 ± 0.000
18:3 (ALA)	0.455 ± 0.001	0.459 ± 0.003	0.479 ± 0.001	0.466 ± 0.001	0.466 ± 0.007	0.446 ± 0.002	0.467 ± 0.002	0.446 ± 0.011	0.441 ± 0.004	0.461 ± 0.005	0.478 ± 0.001
18:3 (GLA)	0.024 ± 0.001	0.050 ± 0.004	0.025 ± 0.001	0.024 ± 0.000	0.016 ± 0.000	0.056 ± 0.001	0.018 ± 0.002	0.034 ± 0.002	0.044 ± 0.001	0.029 ± 0.000	0.027 ± 0.000
18:4 (SDA)	0.035 ± 0.003	0.050 ± 0.001	0.030 ± 0.001	0.025 ± 0.007	0.024 ± 0.002	0.064 ± 0.002	0.023 ± 0.011	0.044 ± 0.004	0.049 ± 0.005	0.029 ± 0.001	0.012 ± 0.000
LA % <sup>a</sup>	4.8 ± 0.2	9.9 ± 0.3	5.1 ± 0.7	4.9 ± 0.3	3.3 ± 0.1	11.1 ± 0.1	3.6 ± 0.1	6.8 ± 0.4	8.8 ± 0.4	5.9 ± 0.2	5.3 ± 0.1
ALA % <sup>a</sup>	6.9 ± 0.2	10 ± 0.6	1.1 ± 0.1	4.9 ± 0.3	4.8 ± 1.4	12.8 ± 0.4	4.6 ± 0.3	8.8 ± 2.3	9.8 ± 0.7	5.8 ± 0.9	2.4 ± 0.3

<sup>a</sup>LA % or ALA % = 100 × ([product] / [product + substrate]).



TABLE 4. Kinetic analysis of each recombinant TpFADS2 and GcFADS2 by mutating amino acids

	Fatty acid	TpFADS2	Mutants									
			V295T	T299S	L303F	I306L	A315S	H360D	F368Y	S377M/L378M	H381N	L383I
$V_{max}^a$	18:2 (LA)	0.40	<b>0.34</b>	0.63	0.48	0.29	<b>0.41</b>	0.34	<b>0.61</b>	<b>1.19</b>	0.44	0.51
	18:3 (ALA)	0.54	<b>0.32</b>	0.83	0.56	0.72	<b>0.27</b>	0.54	<b>0.34</b>	<b>0.91</b>	0.71	0.55
$K_m^a$	18:2 (LA)	187.66	<b>1544.62</b>	627.58	388.28	427.59	<b>1584.02</b>	299.32	<b>2556.04</b>	<b>3547.49</b>	268.73	394.04
	18:3 (ALA)	250.52	<b>1243.70</b>	691.91	495.87	739.78	<b>1464.57</b>	458.76	<b>4412.12</b>	<b>2244.97</b>	521.88	458.13
		Mutants										
$V_{max}^a$	Fatty acid	GcFADS2	T302V	S306T	F310L	L313I	S322A	D367H	Y375F	M384S/M385L	N388H	I390L
	18:2 (LA)	0.12	<b>0.07</b>	0.13	0.13	0.07	<b>0.10</b>	0.09	<b>0.06</b>	<b>0.10</b>	0.22	0.51
$K_m^a$	18:3 (ALA)	0.27	<b>0.07</b>	0.26	0.23	0.12	<b>0.11</b>	0.13	<b>0.07</b>	<b>0.08</b>	0.19	0.16
	18:2 (LA)	1268.06	<b>36.98</b>	1340.53	1399.73	1020.82	<b>159.35</b>	1282.81	<b>106.54</b>	<b>321.97</b>	2182.43	6375.00
	18:3 (ALA)	2315.63	<b>23.87</b>	2621.65	2812.50	1250.00	<b>129.31</b>	1519.23	<b>89.41</b>	<b>123.64</b>	1821.43	4403.13

<sup>a</sup>  $V_{max}$  and  $K_m$  were calculated by the Michaelis-Menten equation. Bold text indicates sites identified to critically influence FADS2 catalytic activity.

FADS2 catalytic activity via induced alterations to their polarity (incurred by the presence of the different amino acids), which may in turn cause changes to the shape of the FADS2-binding pocket that inhibit substrate binding.


The results of the present study also indicate that the C-terminal region located adjacent to the sixth cytoplasmic transmembrane domain (section 9) may significantly influence FADS2 catalytic activity (Figs. 4B, 5B). Furthermore, the result of the second-level assessment of this area revealed that section 9-1 most significantly impacted FADS2 catalytic activity, and only six amino acid sites differ between the GcFADS2 and TpFADS2 9-1 sections. As shown by the results of the analysis of FADS2 catalytic activity in *S. cerevisiae*, the single mutant F368Y and the double mutant S377M/L378M both mediate FADS2 substrate catalysis, likely because the F368 and S377M/L378M residues are located just upstream and downstream of the third conserved FADS2 histidine box, respectively, which is thought to be associated with FADS2 enzymatic and/or substrate binding activity (9). All other mutants did not induce any significant change to the rate of LA and/or ALA conversion, suggesting that their mutated residues are likely located at a distance to the delta 6 C-C substrate bond.

Based on the conducted kinetic analysis, the T302, S322, Y375, and M384/M385 substitutions in TpFADS2 (corresponding to the V295, A315, F368, and S377/L378 substitutions in GcFADS2) significantly impacted FADS2 catalytic efficiency, resulting in the exhibition of low  $K_m$  values by the mutant FADS2s. Thus, these residues likely have strong affinity for LA and ALA under normal conditions.

The present study divided the GcFADS2 and TpFADS2 genes according to their respective transmembrane topologies. The fact that none of the generated chimera sequences exhibited abolished catalytic activity for both substrates suggests that their three-dimensional structures were not disrupted by this division. Although the results of the present study identified several key sites that critically mediate FADS2 catalytic activity, mutation of the majority of these did not affect FADS2 substrate specificity. Mutation of only a few sites, including the TpFADS2 sites I306L and H360D, and the GcFADS2 site I390L, appeared to induce a propensity for FADS2 to favor the binding of a particular fatty acid, suggesting that these may be associated with substrate specificity (Tables 2, 3). Notably, the mutation of these sites did not significantly impact FADS2 catalytic

activity for either substrate, suggesting that they are likely not closely relevant to substrate catalysis. Together, these results suggest that the motifs/residues that mediate FADS2 catalytic activity and substrate specificity are not located in the same region of the FADS2 sequence.

## CONCLUSIONS

Although some organisms have FADS2s capable of high substrate specificity and others have those capable of high catalytic activity, no FADS2 has yet been identified to have both high substrate specificity and high catalytic activity. The present study cloned and characterized the catalytic activity of GcFADS2 and TpFADS2 for both LA and ALA. Reciprocal domain swapping was performed to identify critical regions and, eventually, precise fragments of GcFADS2 and TpFADS2 that mediate FADS2 catalytic activity. Thus, the results of the present study provide valuable insights into the relationship between the primary structure and catalytic activity of delta 6 desaturases. Continued research is required to confirm the FADS2 regions that mediate both its substrate specificity and catalytic activity and to elucidate the molecular mechanisms underlying these processes, enabling, in turn, a better understanding of PUFA metabolism and  $\omega$ 3-PUFA (e.g., EPA and DHA) production. 

## REFERENCES

- Xue, Z., P. L. Sharpe, S-P. Hong, N. S. Yadav, D. Xie, D. R. Short, H. G. Damude, R. A. Rupert, J. E. Seip, and J. Wang. 2013. Production of omega-3 eicosapentaenoic acid by metabolic engineering of *Yarrowia lipolytica*. *Nat. Biotechnol.* **31**: 734–740.
- Gerster, H. 1998. Can adults adequately convert alpha-linolenic acid (18:3n-3) to eicosapentaenoic acid (20:5n-3) and docosahexaenoic acid (22:6n-3)? *Int. J. Vitam. Nutr. Res.* **68**: 159–173.
- Burdge, G. 2004. alpha-linolenic acid metabolism in men and women: nutritional and biological implications. *Curr. Opin. Clin. Nutr. Metab. Care.* **7**: 137–144.
- Zhu, B. H., C. C. Tu, H. P. Shi, G. P. Yang, and K. H. Pan. 2017. Overexpression of endogenous delta-6 fatty acid desaturase gene enhances eicosapentaenoic acid accumulation in *Phaeodactylum tricorutum*. *Process Biochem.* **57**: 43–49.
- Zhou, X-R., S. Robert, S. Singh, and A. Green. 2007. Heterologous production of GLA and SDA by expression of an *Echium plantagineum* Delta 6-desaturase gene. *Plant Sci.* **172**: 421–422.
- Qi, B., T. Fraser, S. Mugford, G. Dobson, O. Sayanova, J. Butler, J. A. Napier, A. K. Stobart, and C. M. Lazarus. 2004. Production of

- very long chain polyunsaturated omega-3 and omega-6 fatty acids in plants. *Nat. Biotechnol.* **22**: 739–745.
- Pou, A., J. L. Abad, Y. F. Ordonez, M. Garrido, J. Casas, G. Fabrias, and A. Delgado. 2017. From the configurational preference of dihydroceramide desaturase-1 towards delta(6)-unsaturated substrates to the discovery of a new inhibitor. *Chem. Commun. (Camb.)*. **53**: 4394–4397.
  - Yary, T., S. Voutilainen, T. P. Tuomainen, A. Ruusunen, T. Nurmi, and J. K. Virtanen. 2017. Omega-6 polyunsaturated fatty acids, serum zinc, delta-5 and delta-6-desaturase activities and incident metabolic syndrome. *J. Hum. Nutr. Diet.* **30**: 506–514.
  - Shi, H., H. Chen, Z. Gu, Y. Song, H. Zhang, W. Chen, and Y. Q. Chen. 2015. Molecular mechanism of substrate specificity for delta 6 desaturase from *Mortierella alpina* and *Micromonas pusilla*. *J. Lipid Res.* **56**: 2309–2321.
  - Hsiao, T. Y., B. Holmes, and H. W. Blanch. 2007. Identification and functional analysis of a delta-6 desaturase from the marine microalga *Glossomastix chrysoplata*. *Mar. Biotechnol. (NY)*. **9**: 154–165.
  - Iskandarov, U., I. Khozin-Goldberg, and Z. Cohen. 2010. Identification and characterization of  $\Delta 12$ ,  $\Delta 6$ , and  $\Delta 5$  desaturases from the green microalga *Parietochloris incisa*. *Lipids*. **45**: 519–530.
  - Kajikawa, M., K. T. Yamato, Y. Kohzu, M. Nojiri, E. Sakuradani, S. Shimizu, Y. Sakai, H. Fukuzawa, and K. Ohyama. 2004. Isolation and characterization of  $\Delta 6$ -desaturase, an ELO-like enzyme and  $\Delta 5$ -desaturase from the liverwort *Marchantia polymorpha* and production of arachidonic and eicosapentaenoic acids in the methylotrophic yeast *Pichia pastoris*. *Plant Mol. Biol.* **54**: 335–352.
  - Kim, S. H., J. B. Kim, S. Y. Kim, K. H. Roh, H. U. Kim, K-R. Lee, Y. S. Jang, M. Kwon, and J. S. Park. 2011. Functional characterization of a delta 6-desaturase gene from the black seabream (*Acanthopagrus schlegelii*). *Biotechnol. Lett.* **33**: 1185–1193.
  - Domergue, F., A. Abbadi, U. Zähringer, H. Moreau, and E. Heinz. 2005. In vivo characterization of the first acyl-CoA Delta6-desaturase from a member of the plant kingdom, the microalga *Ostreococcus tauri*. *Biochem. J.* **389**: 483–490.
  - Zhang, Q., M. Li, H. Ma, Y. Sun, and L. Xing. 2004. Identification and characterization of a novel  $\Delta 6$ -fatty acid desaturase gene from *Rhizopus arrhizus*. *FEBS Lett.* **556**: 81–85.
  - Zhang, R., Y. Zhu, L. Ren, P. Zhou, J. Hu, and L. Yu. 2013. Identification of a fatty acid  $\Delta 6$ -desaturase gene from the eicosapentaenoic acid-producing fungus *Pythium splendens* RBB-5. *Biotechnol. Lett.* **35**: 431–8.
  - Fu, C., Y. R. Chai, L. J. Ma, R. Wang, K. Hu, J. Y. Wu, J. N. Li, X. Liu, and J. X. Lu. 2017. Evening primrose (*Oenothera biennis*) Delta 6 fatty acid desaturase gene family: cloning, characterization, and engineered GLA and SDA production in a staple oil crop. *Mol. Breed.* **37**: 83.
  - Lin, Z. D., M. L. Hao, D. S. Zhu, S. K. Li, and X. B. Wen. 2017. Molecular cloning, mRNA expression and nutritional regulation of a Delta 6 fatty acyl desaturase-like gene of mud crab, *Scylla paramamosain*. *Comp. Biochem. Physiol. B Biochem. Mol. Biol.* **208**: 29–37.
  - Wang, H., M. G. Klein, H. Zou, W. Lane, G. Snell, I. Levin, K. Li, and B-C. Sang. 2015. Crystal structure of human stearyl-coenzyme A desaturase in complex with substrate. *Nat. Struct. Mol. Biol.* **22**: 581–585.
  - Bai, Y., J. G. McCoy, E. J. Levin, P. Sobrado, K. R. Rajashankar, B. G. Fox, and M. Zhou. 2015. X-ray structure of a mammalian stearyl-CoA desaturase. *Nature*. **524**: 252–256.
  - Shi, H., H. Chen, Z. Gu, H. Zhang, W. Chen, and Y. Q. Chen. 2016. Application of a delta-6 desaturase with  $\alpha$ -linolenic acid preference on eicosapentaenoic acid production in *Mortierella alpina*. *Microb. Cell Fact.* **15**: 117.
  - Tonon, T., O. Sayanova, L. V. Michaelson, R. Qing, D. Harvey, T. R. Larson, Y. Li, J. A. Napier, and I. A. Graham. 2005. Fatty acid desaturases from the microalga *Thalassiosira pseudonana*. *FEBS J.* **272**: 3401–3412.